Geometric Optimisation of Electroadhesive Actuators Based on 3D Electrostatic Simulation and its Experimental Verification

J. Guo*, T. Bamber, T. Hovell, M. Chamberlain, L. Justham, and M. Jackson

**EPSRC Centre for Innovative Manufacturing in Intelligent Automation, Loughborough University Loughborough, LE11 3TU, UK (e-mail: J.Guo@lboro.ac.uk)*

Abstract: A systematic research methodology for the performance evaluation of different electroadhesive pad geometries is demonstrated in this paper. The proposed research method for the investigation was based on a 3D electrostatic simulation using COMSOL Multiphysics, a cost-effective electroadhesive pad design and manufacturing process based on solid-ink printing, chemical etching, conformal coating, and an advanced and mechatronic electroadhesive force testing platform and procedure. The method has been validated using 2 novel pad designs, approximate 21 cm x 19 cm, compared with the normal comb design, on the glass and aluminium plate. The experimental results showed that: 1) on the glass substrate, a relative increase of 1% and 28% in the electroadhesive forces obtainable can be seen in the curve-comb pad and the worm-comb pad respectively; and 2) on the Al substrate, a relative increase of 5% and 12% can be seen. This manifests that the two new pad designs, especially the worm-comb shape design, are better at generating larger electroadhesive forces. The comparison between the simulation results and experimental results proved that proposed method is promising for evaluating the pad design before spending time and money on pad manufacture and testing.

Keywords: Electroadhesion, Electroadhesive design and manufacture, Electroadhesive force testing, Geometric optimisation, 3D electrostatic simulation.

1. INTRODUCTION

Electroadhesion is an electrostatic attractive effect between two objects: the electroadhesive pad or electroadhesor and the substrate to which the pad is to be attached onto, when subjected to strong electrical fields (usually in kV mm^{-1} range) [1]. The principle of electroadhesive force generation on conductive and insulating substrate materials is different [2]. For conductive substrates, the electroadhesive forces are generated mainly by electrostatic induction. For insulating substrates, the electroadhesive forces are generated mainly by electric polarization [3].

Electroadhesion has been extensively used as an advanced adhesion method as, compared with other adhesion mechanisms [4], it features an enhanced adaptability, gentle handling, reduced complexity, and ultra-low energy consumption [5]. Electroadhesion is a multidisciplinary, complicated, and dynamic electrostatic attraction phenomenon with over 33 variables influencing the obtainable electroadhesive forces between the electroadhesive pad and the substrate based on the literature survey [6]. Pad geometry or the electrode pattern is one of the major factors influencing the obtainable electroadhesive forces. Various attempts have been made to investigate the performance of different pad geometries for electroadhesive applications [7][8][9]. Simulation and experimental results have both showed that the pad geometry design is essential to achieve both the maximum electroadhesive force [7][10] and fastest clamp/unclamp speed [11][12]. New and novel pad geometries are still desirable for different electroadhesive applications. Also, a comprehensive comparison of some major pad designs stated in the literature review is still needed. It is therefore necessary to continue answering the following two questions: 1) which pad geometry can help produce the maximum electroadhesive force on conductive substrates and non-conductive substrates, and 2) which pad geometry can achieve the fastest clamping and unclamping speed, especially on non-conductive substrates.

This paper is intended to propose a systematic research methodology for the performance evaluation of different electroadhesive pad geometries. The research method for the investigation is based on a 3D electrostatic simulation, a cost-effective electroadhesive pad design and manufacturing process, and an advanced mechatronic electroadhesive force testing platform and procedure. Initial results on the investigation into the relationship between the electroadhesive forces obtainable and different pad geometries are reported.

2. RESEARCH METHODOLOGY

The main aim of the research presented in this paper is: to identify the relationship between the electroadhesive forces obtainable and different pad geometries. To this end, four major research stages have been addressed, as identified in Fig. 1. The first stage of this research was to design the pad geometry in 3D using SOLIDWORKS and to assemble the designed pad with the substrate into an electroadhesive system. After this, a 3D electrostatic simulation was conducted using COMSOL Multiphysics 5.0 to obtain the

overall capacitance of each pad design for comparison. Then, experimental validation was conducted using an advanced and reconfigurable electroadhesive force testing platform. Finally, a correlation between the simulation results and the experimental results was performed.

3. 3D ELECTROSTATIC SIMULATION USING COMSOL

3D electrostatic simulation is useful as it can identify the 3D electric field distribution, field strength, and total energy of each pad geometry (thus can help calculate which pad geometry can output the largest capacitance) without pad manufacturing and testing. This means less cost and time can be spent on pad manufacturing and performance testing.

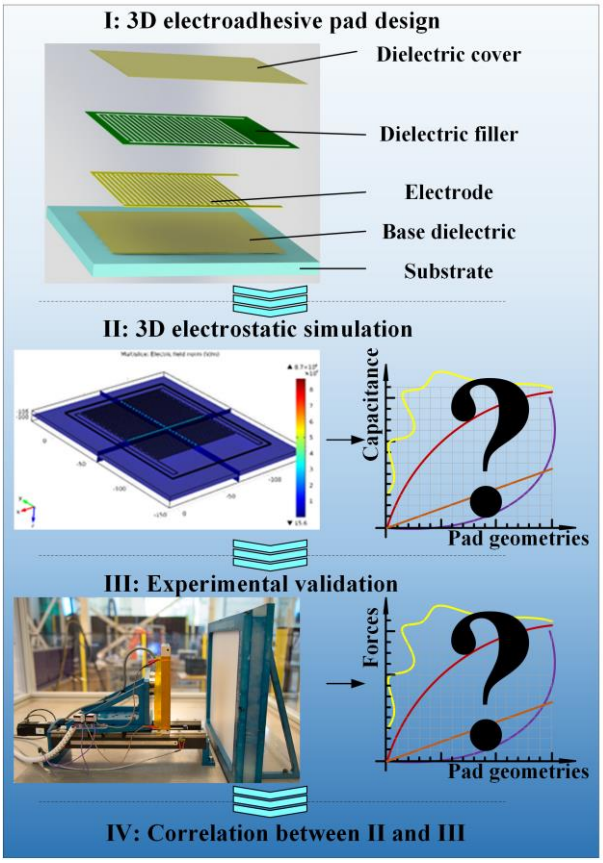

Fig. 1. Research methodology.

3.1 3D electroadhesive pad design

Although various pad designs have already been investigated [7][8][9], only 9 pad designs, including two novel pad designs, were selected for comparison in this paper. A 3D electroadhesive system, including the pad and the substrate assembly together, was created before the 3D electrostatic simulation. In order to only vary the pad geometry, the same substrate with the same dimensions was used. Also, the same base dielectric, dielectric filler, and cover were used to ease the process of material addition. The front view of the 9 pad designs can be seen in Fig. 2, where (a) is the interdigitated or comb shape, (b) is the snake-electrode shape, (c) is the serpentine-electrode shape, (d) is the curve-comb shape, (e) is the worm-comb shape, (f) is tooth-comb shape, (g) is the concentric shape, (h) is the spiral shape, and (i) is the double-electrode shape. (c), (d), (e), and (f) are novel designs for electroadhesive applications.

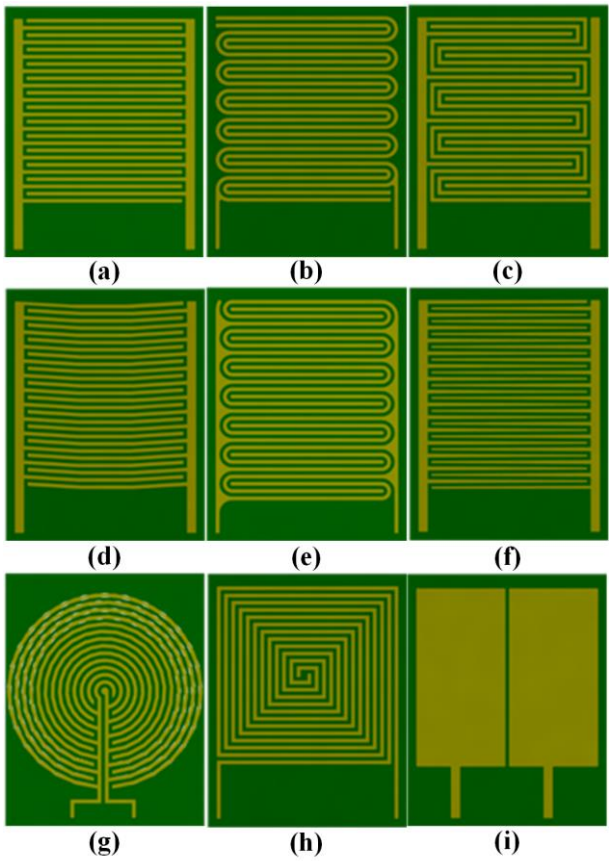

Fig. 2. Pad designs.

3.2 3D electrostatic simulation procedures

The 3D electrostatic simulation procedure can be seen in Fig. 3. The 3D component was added before adding the assembled electroadhesive system from SOLIDWORKS using the LiveLink function in COMSOL. Then the material of each part of the assembled electroadhesive system was added. For the copper electrodes, the dielectric constant was set as 10000; for the glass substrate (quartz), the dielectric constant was set as the default value 4.2; for the dielectric material, Polyimide (PI, Kapton H) was selected and 3.5 was set as its dielectric constant.

Electrostatics was selected when adding physics into the model. After this, the boundary conditions of the model were set. For all the pad designs, the left electrode was set with an electric potential of 3000 V; the right electrode was set with an electric potential of -3000 V; and the bottom face of the substrate was set with an electric potential of 0 V.

Finite element method is not good at dealing with high-aspect ratio systems such as the multi-layer thin film based electroadhsion system. Simplification should be made in order to have a successful mesh and computation. The

dimensions of the substrate were all set as 10 mm (thickness) x 150 mm x 180 mm. The electrode thickness does not generate significant influence on the electroadhesive forces obtainable [10]. Therefore, in order to quickly have a successful mesh, the electrode thickness, and thickness of the base dielectric and dielectric cover were all set as 0.5 mm. After the mesh, a stationary study was added to the model. The results were obtained after the computation and data post-processing. The 3D electric field distribution of the selected pad geometries on glass in COMSOL is presented in Fig. 4.

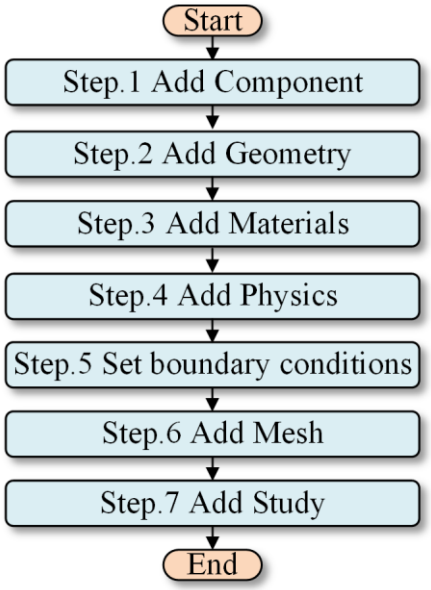

Fig. 3. Simulation procedures.

3.3 3D electrostatic simulation results

In order to compare the pad geometry, the total capacitance for each pad geometry (the simulation result) can be derived. The larger the total capacitance, the larger the electroadhesive forces will be generated by the pad. In COMSOL, the total capacitance can be derived from the following expression:

$$C = \frac{2W_e}{V^2}$$

where W_e is the total electric energy of the electroadhesive system and V is the voltage applied across the electrodes.

The total capacitance generated by each pad geometry on the glass substrate from the COMSOL simulation is presented in Fig. 5. From the results shown in Fig. 5, the novel worm-comb shape generates the largest total capacitance on the glass, whereas the double-electrode shape generates the lowest total capacitance on glass. There is a 540% relative increase between the double-electrode shape and the novel worm-comb shape. This means that the pad geometry does generate a significant difference on the obtainable electroadhesive forces on non-conductive substrates such as the glass. Also, it is interesting to note that among the five comb shapes, i.e. the geometry a, c, d, e and f, only a 10% relative difference can be seen. Geometry b generates a lower total capacitance on the glass than the comb shapes. This is similar to the results obtained by Savioli et al. [13].

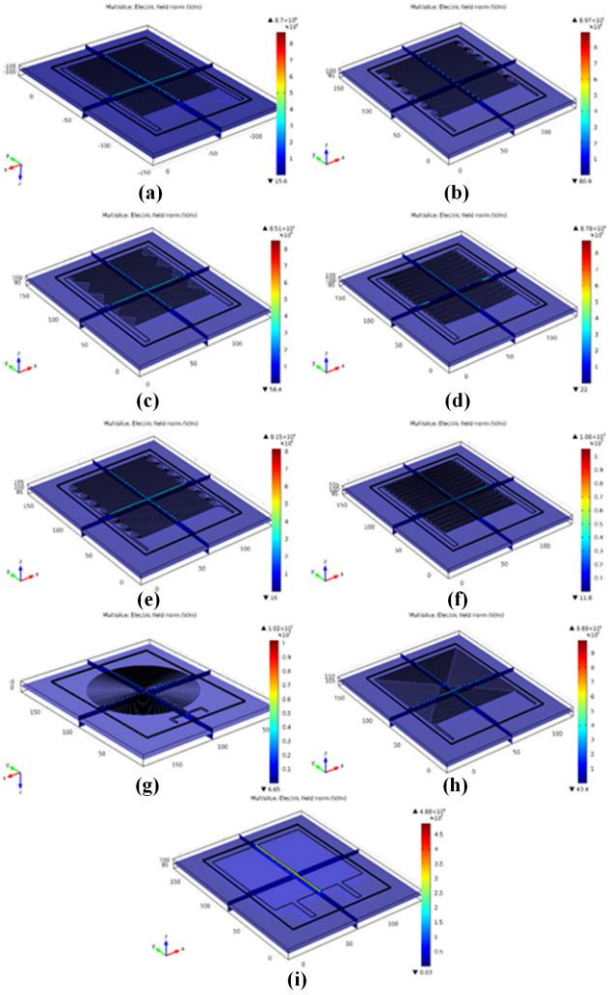

Fig. 4. 3D electric field distribution of the selected pad geometries on glass in COMSOL.

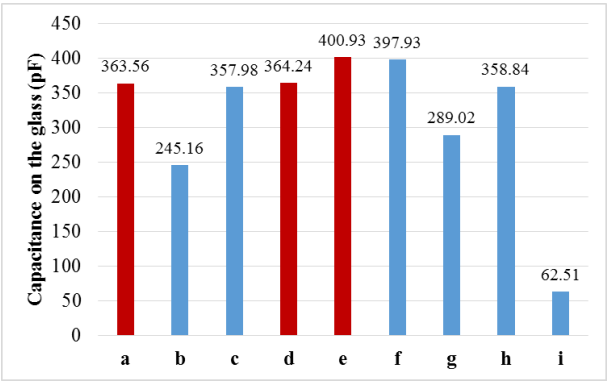

Fig. 5. Capacitance of the electroadhesion systems on the glass.

It seems that the concentric shape is not necessarily superior to the comb shapes, which is different from the results

obtained by Ruffatto et al. [10]. This may be because that varying electrode widths were not adopted here but this requires a further and systematic experimental validation. Also, for the concentric design, the radius was 50 mm, the effective area was therefore 21.5% smaller.

The total capacitance generated by each pad geometry on the aluminium (the default Al in COMSOL) substrate is presented in Fig. 6. The dielectric constant of this material was set as 10000. It is demonstrated in Fig. 6 that most of the pad geometries (a, b, d, e, f, and h) have a relative decrease of approximately 24% compared with the total capacitance obtained from the glass substrate.

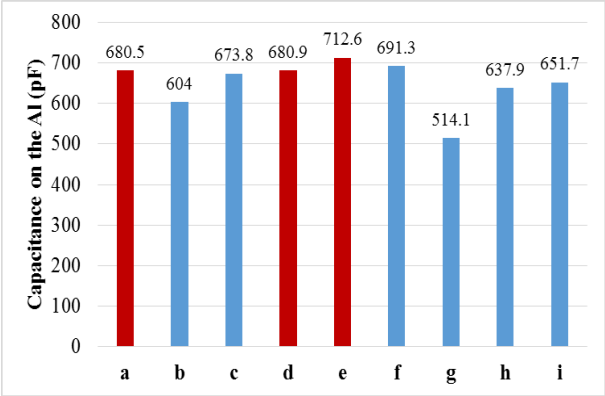

Fig. 6. Capacitance of the electroadhesion systems on the Al.

4. EXPERIMENTAL VERIFICATION

Experimental validation is vital to check whether the proposed is correct. It is desirable that the experimental results can agree with the simulation results as this will lead to less pad manufacturing and experimental testing, thus a more cost-effective and efficient process can be achieved in the future for novel pad geometry investigation. In this paper, an initial experimental validation was conducted to compare the two novel designs, the curve-comb shape (design d) and the worm-comb shape (design e), with the standard comb shape design (design a).

4.1 Pad design and manufacture

The pads were manufactured using the steps shown in Fig. 7, where a cost-effective in house pad design and manufacturing method based on the solid ink printing technique, chemical etching, and conformal coating was employed. The specific steps for the pad design and manufacture process are summarised below:

Step 1: Copper laminate preparation

The roll of copper laminate was cut by a cutter into A4 sized pads. The edges of the A4 pads were smoothed with sand paper to remove any burrs or jagged edges to prevent catching within the printer. The pads were then cleaned using Iso-Propyl Alcohol (IPA) and acetone to remove any contaminants to ensure a clean surface for the wax to adhere to. The copper laminate was made of a 20 µm copper adhered on a 23 µm Polyester (PET, dielectric strength: 310 kV/mm, dielectric constant: 3.2)

Step 2: Electroadhesive pad geometry design

All the pads were designed in Solidworks. The effective electrode area of the pad was designed to be 176 mm x 228 mm. The electrode width and space between electrodes were designed to be 1.8 mm and 4 mm respectively.

Step 3: Protective wax printing based on the pad design using a solid-ink printer

The dried A4 pad was loaded into a Xerox solid-ink printer. A protective layer of wax was then printed on the copper side of the copper laminate based on the pad design.

Step 4: Chemical etching

The pad was then placed into a heated bubble etching tank where ferric chloride granules dissolved in water removed the unprotected copper areas leaving the protected wax regions behind.

Step 5: Wax removal and cleaning the etched pad

Once the etching was completed any excess chemical acid was washed off using a water bath. The wax was then removed by applying a label removal. After this, the pad was cleaned using IPA and acetone again

Step 6: Dielectric material filling using conformal coating

After drying the pad, the pad was held flat using a spray pad holder. The conformal spraying of an aerosol of Polyurethane (PUC, dielectric strength: 60 kV/mm, dielectric constant: 3.6) was carried out in a spray booth.

Step 7: Degassing and curing

Once an even coat was applied to the surface of the pad, the pad was placed into a vacuum oven. Once inside, the vacuum was applied to pull out any air bubbles that were within the dielectric. As soon as bubbles were no longer appearing on the surface of the dielectric the oven was turned on and set to 80 ^{o}C and the pad left to cure inside for 90 minutes.

Once the dielectric was cured, the pad was taken out of the oven. The quality of the dielectric covering was then inspected for contaminants, distribution evenness, and areas that were not covered by any dielectric. The cured pad was then left to cool down overnight to ensure that there was no tackiness to the dielectric which would cause it to adhere to the pad holder or substrate.

4.2 Electroadhesive force testing

A mechatronic and reconfigurable electroadhesive force measurement platform was used to obtain the normal electroadhesive forces between the pads and substrates. The system diagram can be seen in Fig. 8 (a), where a 6-axis ATI Gamma Force/Torque (F/T) sensor was used to record the electroadhesive forces.

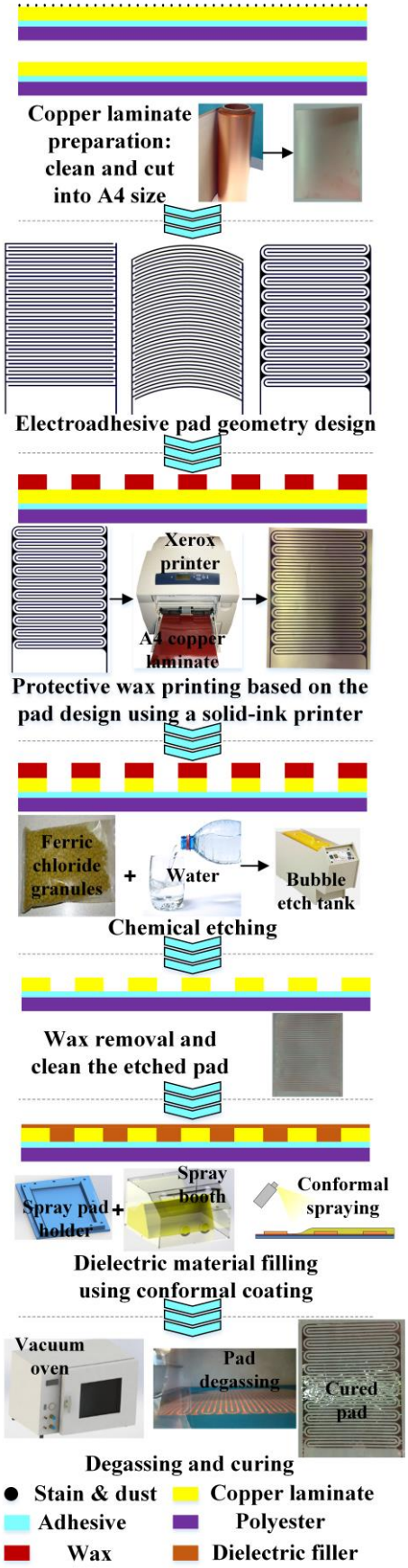

Fig. 7. Pad design and manufacture process.

The communication between the F/T sensor and the computer was through a netbox via an Ethernet cable and the data was selected to be sampled at 152 Hz. The reason why 152 Hz was selected was because the frequency was compatible to an IMU sensor worked together with the F/T sensor for another purpose. The linear rail achieves vertical movement using a servo motor with encoder driven by a Kollmorgen motor driver connected with a CompactRio. This allows almost real time control of the linear rail via a Xilinx FPGA, which is designed to communicate with the computer via Ethernet. The smallest movement of the linear rail that the encoder can recognize is approximately 0.8 μm. The pad was connected with two EMCO high voltage converters with (±) 0-10 kV output and 0-5 V reference input. The reference input was from a direct current power supply unit, an Instek GPD3303, which was designed to communicate with the computer through via USB. The physical setup can be seen in Fig. 8 (b). A Labview interface was developed for interactive control of the movement of the linear rail, changing the supply voltage, recording and saving the electroadhesive force data [6].

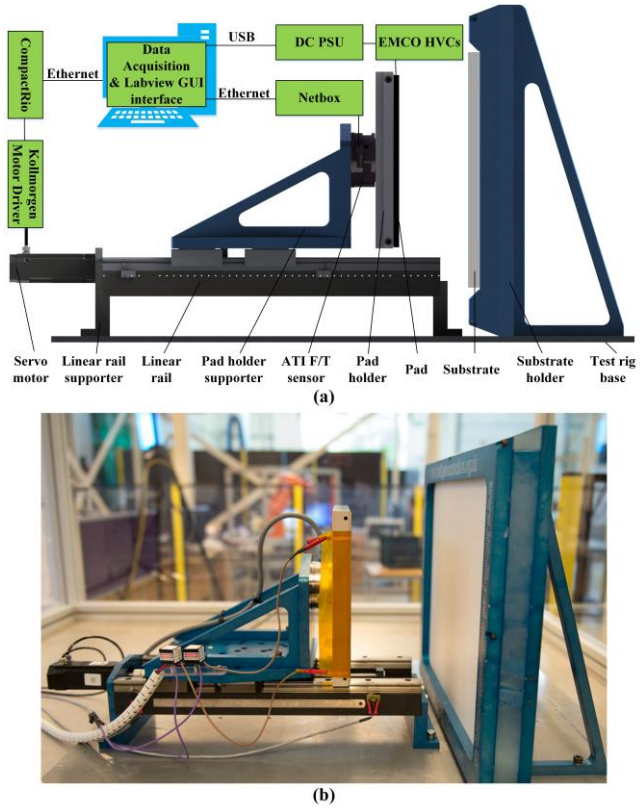

Fig. 8. Electroadhesive force testing platform (a) system diagram and (b) physical setup.

For each pad, five experiments were repeated. The electroadhesive force measurement procedures can be seen in Fig. 9. The pad was initially attached on the pad holder. A 32 N preload was then applied on the substrates. The recording of the electroadhesive forces was then started by turning on the power supply, thus providing power to the pad. The pad was charged for 60 seconds. After this, the pad was pulled away by activating the servo motor. When the motor

stopped, the data recording was completed and the data was exported as text files. These files were filtered and analysed using MATLAB. The next experiment was conducted after 540 seconds dwell time.

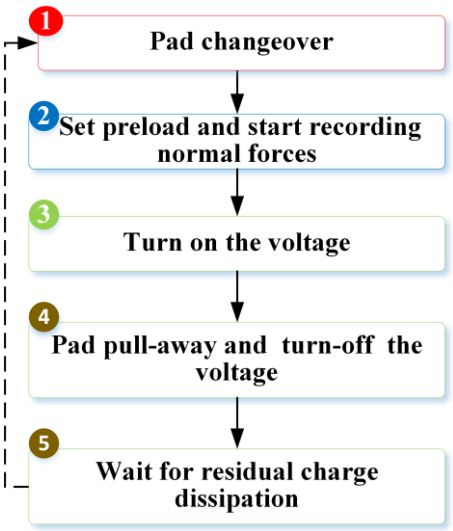

Fig. 9. Electroadhesive force measurement procedures [6].

The dwell time was useful for residual charge dissipation. During the residual charge dissipation process, the pad was grounded for 300 seconds after each test. Also, the aluminium (Al) substrate was grounded for 300 seconds each time before change the pad. An electrostatic fieldmeter, FMX-003, mounted on Kanya frames, was used to compare the surface charge value of the plate before applying the voltage and after the grounding. 300 seconds were enough to obtain similar results that were less than 5% difference. Also, each time after applying the preload, little difference was observed after 10 seconds' stabilising. A fixed experiment time of 10 minutes (540 seconds plus 60 seconds) for each test was therefore set for this investigation [6].

The obtainable electroadhesive forces may change during the day and between days [6]. The experimental validation was therefore conducted based on a temperature/humidity controlled environment. Also, the pads were properly clamped on the pad holder. During the tests, the PET side of the pads was used to face a toughened glass and Al substrate. The pads were charged by applying 3.2 kV for 60 seconds before pulling the pad away from the substrate. The motor pull-off velocity (0.1 mms^{-1}) and pull-off acceleration (50 $revs^{-2}$), charge time (60 s) and discharge time (510 s) were maintained at constant values when conducting the experiments. The experiments were conducted when the relative humidity was 40 $\pm$ 1 %, room temperature was 25 $\pm$ 0.2 °C, and preload was 32 $\pm$ 1 N.

4.3 Experimental results and discussion

The results of the electroadhesive forces obtained by the normal comb shape, the curve-comb shape, and the worm-comb shape pad on the glass and Al substrates can be seen in Fig. 10. On the glass substrate, a relative increase of 1% and 28% in the electroadhesive forces obtainable can be seen in the curve-comb pad and the worm-comb pad respectively. On the Al substrate, a relative increase of 5% and 12% in the electroadhesive forces obtainable can be seen in the curve-comb pad and the worm-comb pad respectively. These results are close to the simulation results, as shown in Fig. 11. This manifests that the proposed method is promising for evaluating the pad design before spending time and money on pad manufacture and testing.

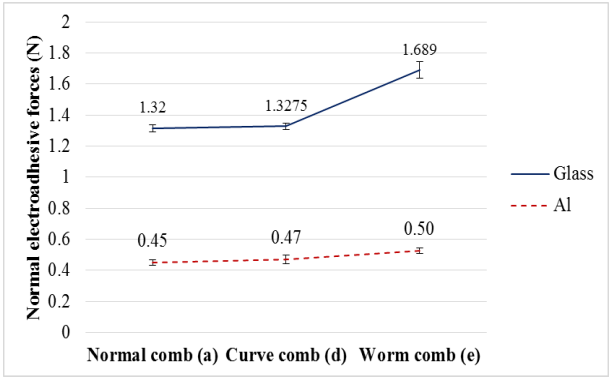

Fig. 10. Comparison of the normal comb, the curve-comb, and the worm-comb pad on the glass and aluminium substrates.

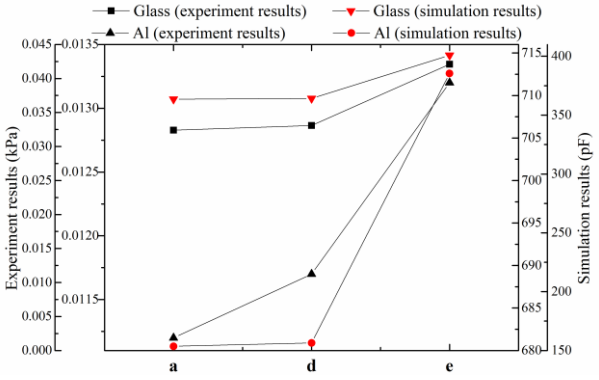

Fig. 11. Trend comparison between the simulation results and the experiment results.

5. CONCLUSIONS

This paper has introduced a systematic research methodology for the performance evaluation of different electroadhesive pad geometries. The investigation was based on 3D electrostatic simulation, a cost-effective electroadhesive pad design and manufacturing process, and an advanced mechatronic electroadhesive force testing platform and procedure. The initial results have validated the feasibility of using 3D electrostatic simulation to optimise the electroadhesive pad design. This will save a significant amount of time and money on pad design, manufacture, and testing. The presented two novel pad designs, the curve-comb shape and the worm-comb shape design, showed that, compared with the normal comb shape design, a relative increase of 1% and 28% in the electroadhesive forces

obtainable on the glass substrate and a relative increase of 5% and 12% on the Al plate can be seen. This manifests the two novel designs, especially the worm-comb shape design, are better at generating larger electroadhesive forces. Although the proposed research methodology is promising, more in-depth simulation and comprehensive experimental validation of all the presented designs are required.

The optimised electroadhesive pad is useful for the industrial material handling application such as pick-and-place of aluminium plates, carbon fibres, and wax that the authors has been investigating.

ACKNOWLEDGEMENT

The authors acknowledge support from the EPSRC Centre for Innovative Manufacturing in Intelligent Automation, in undertaking this research work under grant reference number EP/IO33467/1.

REFERENCES

[1] R. P. Krape, “Application studies of electroadhesive devices,” Springfield (National Aeronautics and Space Administration), 1968.
[2] G. J. Monkman, “An analysis of astrictive prehension,” Int. J. Robot., vol. 16, no. 1, pp. 1–10, 1997.
[3] D. Ruffatto, J. Shah, and M. Spenko, “Increasing the adhesion force of electrostatic adhesives using optimized electrode geometry and a novel manufacturing process,” J. Electrostat., vol. 72, no. 2, pp. 147–155, 2014.
[4] J. L. Guo, L. Justham, M. Jackson, and R. Parkin, “A concept selection method for designing climbing robots,” Key Eng. Mater., vol. 649, pp. 22–29, 2015.
[5] “Grabit Inc.” [Online]. Available: https://grabitinc.com/. [Accessed: 28-Jan-2016].
[6] J. Guo, M. Tailor, T. Bamber, M. Chamberlain, L. Justham, and M. Jackson, “Investigation of relationship between interfacial electroadhesive force and surface texture,” J. Phys. D. Appl. Phys., vol. 49, no. 3, p. 35303(9pp), 2016.
[7] J. P. D. Téllez, J. Krahn, and C. Menon, “Characterization of electro-adhesives for robotic applications,” in IEEE International Conference on Robotics and Biomimetics (ROBIO), 2011, pp. 1867–1872.
[8] D. Ruffatto, J. Shah, and M. Spenko, “Optimization and experimental validation of electrostatic adhesive geometry,” in 2013 IEEE Aerospace Conference, 2013, pp. 1–8.
[9] J. Germann, M. Dommer, R. Pericet-Camara, and D. Floreano, “Active connection mechanism for soft modular robots,” Adv. Robot., vol. 26, no. 7, pp. 785–798, 2012.
[10] D. Ruffatto, J. Shah, and M. Spenko, “Optimization of electrostatic adhesives for robotic climbing and manipulation,” in Proceedings of the ASME 2012 International Design Engineering Technical Conferences & Computers and Information in Engineering Conference, 2012, pp. 1–10.
[11] K. Yatsuzuka, F. Hatakeyama, K. Asano, and S. Aonuma, “Fundamental characteristics of electrostatic wafer chuck with insulating sealant,” IEEE Trans. Ind. Appl., vol. 36, no. 2, pp. 510–516, 2000.
[12] K. Asano, F. Hatakeyama, and K. Yatsuzuka, “Fundamental study of an electrostatic chuck for silicon wafer handling,” IEEE Trans. Ind. Appl., vol. 38, no. 3, pp. 840–845, May 2002.
[13] L. Savioli, G. Sguotti, A. Francesconi, F. Branz, J. Krahn, and C. Menon, “Morphing electroadhesive interface to manipulate uncooperative objects,” in Sensors and Smart Structures Technologies for Civil, Mechanical, and Aerospace Systems 2014, 2014, vol. 9061, p. 906129(13pp).